Matrix Infrared Spectra and Density Functional Calculations of Three Al, N, O Isomers

Lester Andrews,* Mingfei Zhou, and William D. Bare

Department of Chemistry, University of Virginia, Charlottesville, Virginia 22901

Received: January 23, 1998; In Final Form: March 26, 1998

Laser-ablated aluminum atoms have been reacted with NO, ^{15}NO, and $^{15}N^{18}O$ during condensation in excess argon using a variety of concentrations and laser energies/cm^2. Four of the five major product absorptions with higher laser energy were also observed with lower laser energy. The isotopic frequency ratios characterize different normal modes, and these are uniquely matched to the stretching modes of triplet AlON (1282.1, 566.7 cm^{-1}) and triplet AlNO (1644.3, 510.2 cm^{-1}) by density functional theory (DFT) isotopic frequency calculations. The fifth band (1079.5 cm^{-1}) is due to a terminal Al−O stretching mode that is consistent with triplet NAlO based on DFT isotopic frequency calculations. The total product yield depended on laser energy; both AlON and AlNO addition products were produced with lower energy, but the insertion product NAlO required higher energy. Anions were favored with lower laser energy, and a weak 1380.6 cm^{-1} band is assigned to $AlNO^-$ in accord with DFT isotopic frequency calculations.

Introduction

Aluminum is a major element in materials of construction, and accordingly it is important to understand aluminum reactions with oxygen and nitrogen. The emergence of aluminum nitride as a semiconductor and ceramic material[1] prompted a study of laser-ablated aluminum atom reactions with nitrogen in this laboratory.[2] Owing to the unusual thermodynamic stability of aluminum oxides, the possibility of oxygen contamination in aluminum/nitrogen systems must be considered. One method for controlled oxygen addition to the aluminum/nitrogen system is to react Al with NO diluted in N_2. A matrix isolation study of laser-ablated Al atom reactions with NO was carried out for these reasons.

A report of thermal Al atom reactions with NO in excess argon by Ruschel and Ball revealed a new 1282 cm^{-1} absorption, which was suggested to arise from AlON instead of AlNO based on the ^{15}NO shift to 1263 cm^{-1} and quantum chemical calculations.[3,4] This question of nitrosyl vs. nitroxide stability for a matrix-isolated metal atom/nitric oxide reaction product was first addressed by Andrews and Pimentel for lithium.[5]

Laser-ablated aluminum atoms have been reacted with O_2, H_2, C_2H_2, NH_3, and HCN in this laboratory.[6−10] Perhaps the most interesting and relevant reaction is the insertion into oxygen to form the linear OAlO dioxide, a reaction that requires activation energy, in contrast to the addition reaction to form cyclic Al(O_2), a reaction that proceeds on annealing in solid argon.[6] We are interested in understanding the mechanism of reactions of laser-ablated atoms, and accordingly report here a detailed investigation of the reaction of laser-ablated Al atoms with NO, ^{15}NO, and $^{15}N^{18}O$ during condensation in excess argon. We will show by comparison of isotopic frequencies observed for two stretching modes and those calculated by density functional theory (DFT)/B3LYP that the major product is AlON, and that the other addition product, AlNO, is also formed. Under proper conditions the insertion product, NAlO, is also produced and trapped. The vibrational mechanics of each of these structural isomers is different, and the normal modes for each molecule are uniquely described by isotopic substitution in the observed and calculated frequencies.

Experimental Section

The laser-ablation matrix isolation experiment and apparatus have been described in previous reports.[6−10] An aluminum target (Aesar, 99.998%) positioned 2 cm from the cold window was ablated by focused 1064 nm radiation from a pulsed YAG laser. Nitric oxide (Matheson) samples were prepared after fractional distillation from a coldfinger; ^{15}NO (MSD Isotopes, 99% ^{15}N) was treated similarly; $^{15}N^{18}O$ (Isotec, 99.9% ^{15}N, 98.5% ^{18}O) was used as received. A 1:1 mixture of $^{14}N^{16}O$ and $^{15}N^{18}O$ in a stainless steel cylinder quickly equilibrated to a 1:1:1:1 mixture of $^{14}N^{16}O$, $^{15}N^{16}O$, $^{14}N^{18}O$, $^{15}N^{18}O$. A Nicolet 750 FTIR instrument operating at 0.5 cm^{-1} resolution (frequency accuracy ±0.1 cm^{-1}) with liquid nitrogen-cooled MCTB detector was used to record spectra. The instrument was purged continuously with a Balston 75-20 compressed air-dryer. Matrix samples were codeposited on a 10 K CsI window and were temperature cycled from 10 K to allow diffusion and reaction of trapped species, then more spectra were collected.

Results

Five experiments were done with 0.2% NO in argon using different laser energies and focus spot sizes (i.e., different Al atom concentrations and energies), and spectra from two of these experiments are shown in Figures 1 and 2 for selected wavenumber regions. Sample deposition at 10 K for 1 h using focused (0.2 mm diameter spot) laser power on the order of one GW/cm^2 with a bright blue plume reveals the spectrum in Figure 1 and the new bands listed in Table 1. Note sharp doublets (labeled AlON) at 1282.1, 1276.4 and 576.4, 566.7 cm^{-1}. These bands increase together (+80%) on annealing to 25 K (Figure 1 a,b), increase together (+20%) on broadband photolysis, which favors the weaker components (sites in Table 1) (Figure 1c). Further annealing to 30 K increases the stronger bands (+70%) and reduces the weaker bands (−60%) (Figure 1d). Another annealing to 35 K (Figure 1e) increases the major bands by 10% and eliminates the minor bands. Another pair of doublets at 1647.4, 1644.3 and 515.4, 510.2 cm^{-1} exhibits

S1089-5639(98)00858-5 CCC: $15.00
Published on Web 06/09/1998

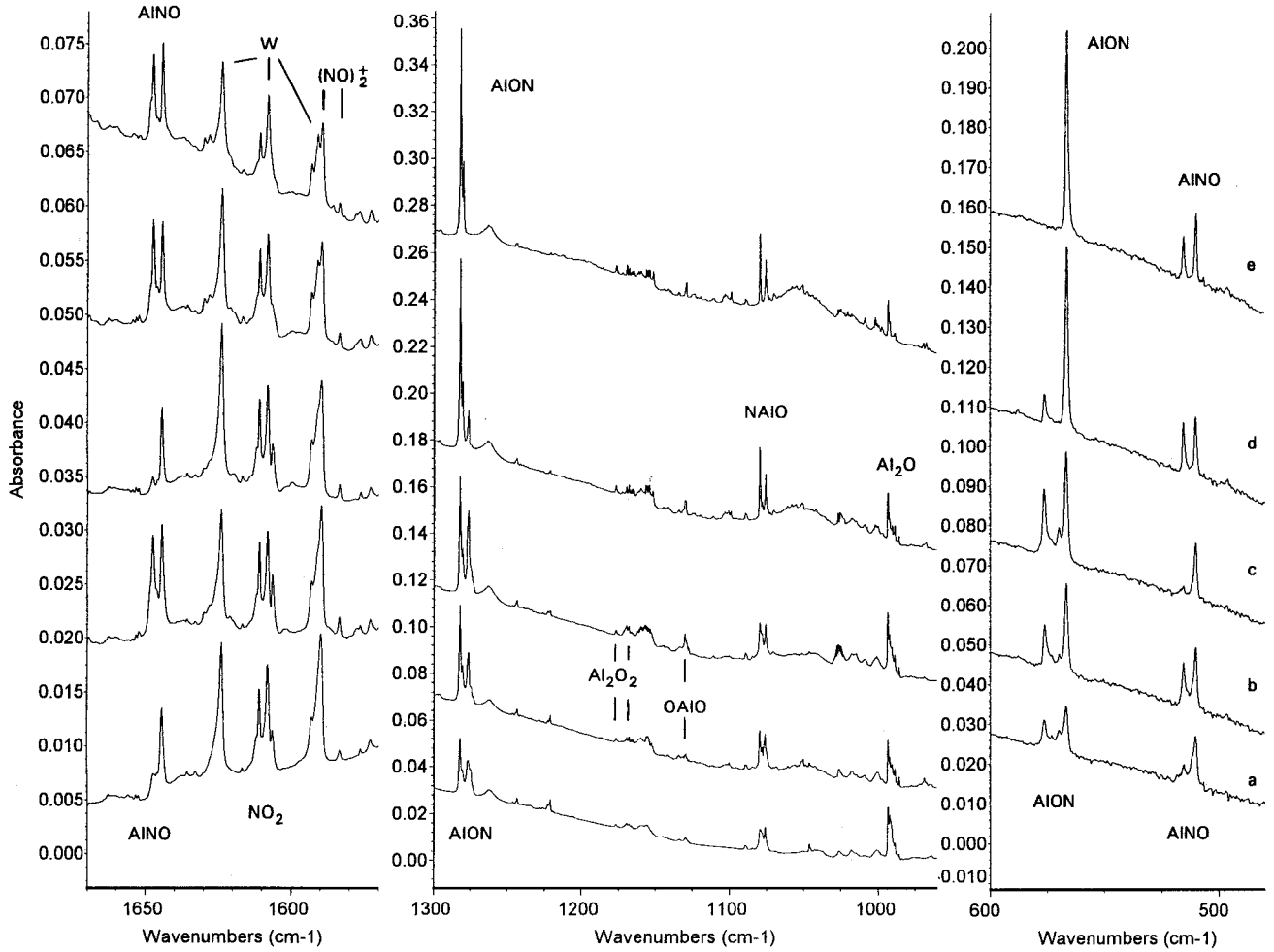

Figure 1. Infrared spectra in selected regions for laser-ablated Al atoms (higher power, 0.2 mm spot) codeposited with 0.2% NO in excess argon on a 10 K CsI window; (a) spectrum after 1 h sample codeposition at 10 K, (b) spectrum after annealing to 25 K, (c) spectrum after broadband photolysis for 30 min, (d) spectrum after annealing to 30 K, and (e) spectrum after annealing to 35 K.

different behaviors for each component. In general, the upper component increases on annealing and decreases on photolysis much more than the lower component. A doublet at 1079.5, 1075.8 cm^{-1} sharpens and increases (+50%) on annealing to 25 K, is essentially unchanged on photolysis, sharpens and increases (+50%) on 30 K annealing, and holds fast on 35 K annealing. A weak band at 1380.6 cm^{-1} (half the absorbance at 1644.3 cm^{-1}) decreased on annealing to 25 K and was destroyed on photolysis, never to return on further annealing. The 2218.5 and 1610.8 cm^{-1} N_2O and NO_2 bands increased by 30% on annealing to 25 K. A final annealing to 40 K slightly decreased the 1282.1 and 566.7 cm^{-1} absorptions, virtually destroyed the 1079.5, 1075.8 cm^{-1} bands, and destroyed the 1647.4 and 515.4 cm^{-1} components without changing the 1644.3 and 510.2 cm^{-1} components of the latter doublet. Sharp, weak 1099.0 and 869.3 cm^{-1} bands appeared together during the annealing sequence. In addition, strong NO, $(NO)_2$ bands, weak NO_2, N_2O, NO_2^-, $Al(O_2)$, OAlO, Al_2O_2, and Al_2O absorptions, and a weak 1589.1, 1583.3 cm^{-1} doublet due to $(NO)_2^+$ were observed.[6,11−14] Weak new bands appeared at 1697.5, 1564.0, 1531.0, 1495.2, 1467.2, and 1421.4 cm^{-1} on annealing, were destroyed by photolysis, and reappeared on further annealing. Annealing also increased weak bands at 1155.8 and 1026.5 cm^{-1}, which are believed to be due to aluminum oxide complexes with precursor. These bands, and aluminum oxide bands, decreased after ablation of surface oxides from the target during the series of experiments.

In contrast, Figure 2 shows the spectrum using 25% of the above focused (0.2 mm diameter spot) laser energy with a very faint plume. The spectrum is cleaner and the product band yield is considerably less as the absorbance scale illustrates. The satellite bands on the major products are also much weaker. The 1282.1, 566.7 cm^{-1} band yield is reduced to 40% but the relative absorbances (0.009−0.005 absorbance units, AU) remained the same, and the 1644.3, 510.2 cm^{-1} absorbances are reduced to 20% of the Figure 1 values, but the relative peak heights (0.0012−0.003 AU) are approximately constant. The 1079.5 cm^{-1} band was barely detected. Annealing increased these band pairs slightly in concert, and photolysis had only a slight effect, similar to the higher power experiment. Again, a weak 1380.6 cm^{-1} band was observed (0.007 AU) which decreased on annealing and photolysis as before.

Another experiment was performed with the focusing lens back 1 cm (2 mm diameter spot) and the same laser energy employed for the experiment reported in Figure 1; the spectrum is similar to that in Figure 2. The absolute yield of the 1644.3 and 510.2 cm^{-1} bands is 15%, and for the 1282.1 and 566.7 cm^{-1} absorptions the absolute yield is 25% with the larger laser spot. The weak 1380.6 cm^{-1} band was equal in absorbance to the 1644.3 cm^{-1} band. The yield of Al_2O was markedly reduced and the 1079.5, 1075.8 cm^{-1} bands were not observed. Although the NO_2 and NO_2^- signals are stronger in Figure 1, the 1221.0 and 1205.3 cm^{-1} bands are *more intense with the lower laser energy*. The 1644.3, 1282.1, 566.7, and 510.2 cm^{-1}

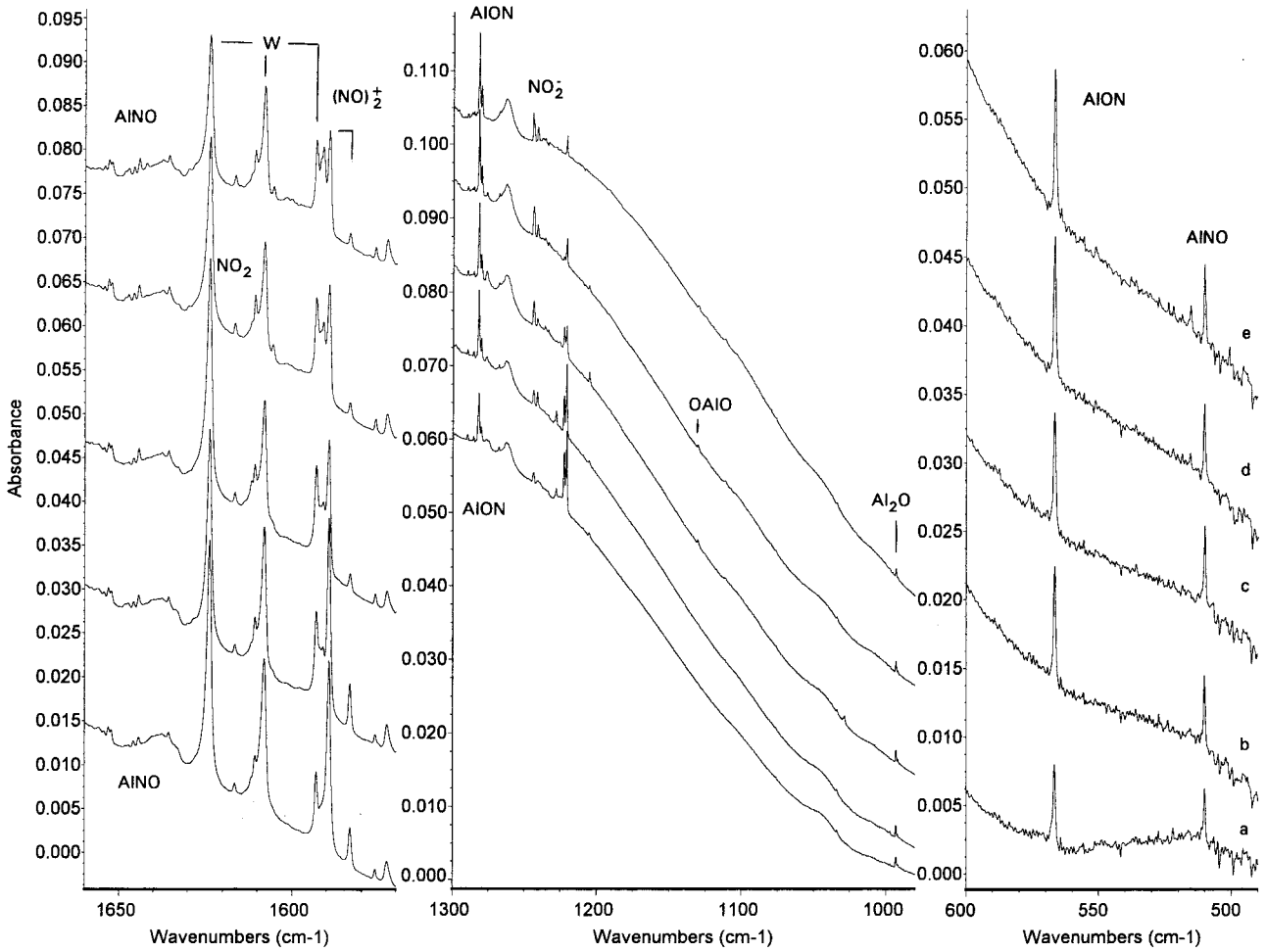

Figure 2. Infrared spectra in selected regions for laser-ablated Al atoms (lower power, 0.2 mm spot) codeposited with 0.3% NO in excess argon on a 10 K CsI window; (a) spectrum after 1 h sample codeposition at 10 K, (b) spectrum after annealing to 25 K, (c) spectrum after broadband photolysis for 30 min, (d) spectrum after annealing to 30 K, and (e) spectrum after annealing to 35 K.

bands exhibited the same annealing and photolysis behavior as described above.

Two experiments with ^{15}NO gave the same behavior with peaks shifted as listed in Table 1. A study with $^{15}N^{18}O$ gave the spectra illustrated in Figure 3. Very weak 1129.9 and 993.0 cm^{-1} bands were observed for $^{16}OAl^{16}O$ and $Al_2^{16}O$ in the deposited sample (Figure 3a) from target surface oxide; stronger ($\times 3$) bands at 1100.8 and 950.2 cm^{-1} for $^{18}OAl^{18}O$ and $Al_2^{18}O$, respectively, show that some dissociative reaction of the precursor occurs. The product doublets show further isotopic shifts as listed in Table 1 and the same annealing behavior described above.

Two experiments were done with mixtures of 14−16, 15−16, 14−18, and 15−18 isotopic NO molecules at a total concentration of 0.5% in argon. Owing to isotopic dilution the strongest bands were favored; quartets were observed at 1644.3, 1612.6, 1607.3, 1574.7; 1282.1, 1263.2, 1244.2, 1224.5; 1079.5, 1077.3, 1047.5, 1044.0; 566.7, 560.9, 560.3, 554.9; and 510.2, 506.7, 501.4, 498.3 cm^{-1}. The components of each isotopic quartet tracked together on annealing. Only pure isotopic components were observed; no evidence was found for mixed isotopic bands, which demonstrates that these absorptions are due to products that contain a single NO molecule. Results from such a mixed experiment with 25% ^{18}O enrichment are shown in Figure 4. The upper region shows the $^{14}N^{16}O$ and $^{15}N^{16}O$ product doublets at 1647.4, 1644.3 and 1615.8, 1612.6 cm^{-1} (labeled AlNO); the weaker $N^{18}O$ counterparts are masked. The strongest absorption gives the evenly spaced quartet at 1282.1, 1263.2, 1244.2, 1224.5 cm^{-1} (labeled AlON). The 1079.5 cm^{-1} band (and site splittings) also gave a quartet (not shown). The sharp band that increased on annealing, at 1098.9 cm^{-1}, was not resolved into pure nitrogen isotopic components, but the 869.3 and 852.1 cm^{-1} bands were detected. The two lower frequency bands in the 500 cm^{-1} region gave essentially pure $^{14}N^{16}O$, $^{15}N^{16}O$ isotopic doublets with weak $^{15}N^{18}O$ counterparts.

Similar experiments were done with Al and N_2O or NO_2 in excess argon. The NO_2 experiment gave a larger yield of the 748.0 cm^{-1} band and the 1243.7 cm^{-1} NO_2^- band relative to the new 1221.0 cm^{-1} feature. Weak NO product bands were observed owing to the photochemical production of NO from NO_2 in the laser ablation experiment. The N_2O experiment gave an increased yield of aluminum oxides, no NO products, no 1221.0 cm^{-1} band, but an increased yield of the NNO_2^- band[11,13] at 1205.3 cm^{-1}.

One experiment was done with 0.5% NO in nitrogen, and the product absorptions for Al reacting with N_2 were observed here as well.[2] In addition, sharp bands at 1282.0, 1275.8 and 564.8, 562.1 cm^{-1} increased 10% on annealing to 25 K, then decreased on annealing to 30 and 35 K. A broader band with sharp 1078.6, 1076.5 cm^{-1} peaks exhibited similar behavior; decrease of the sharp 1078.6, 1076.5 cm^{-1} peaks was accompanied by the growth of sharp 1098.3, 1094.9 cm^{-1} features. A sharp 509.7, 507.6 cm^{-1} doublet decreased ($\times 0.8$) on annealing to 25 K, was restored by broadband UV photolysis, and decreased ($\times 0.8$) on annealing to 30 K; matching behavior

TABLE 1: Product Absorptions (cm^{-1}) in the Reaction of Laser-Ablated Aluminum Atoms with Isotopic Nitric Oxide Molecules in Condensing Argon

14−16	15−16	14−18	15−18	A/P[a]	identification
1871.8	1838.8	1823.2	1789.2	−/o	NO reagent
1697.5	1667.7	−	−	+/−	$Al_x(NO)_y$
1647.4	1616.8	1610 sh	1577.5	+/−	AlNO site
1644.3	1612.6	1607.3	1574.7	+/+	AlNO
1589.1	1561.9		1520.4	−/−	$(NO)_2^+$
1564.0	1536.6		1495.5	+/−	$Al_x(NO)_y$
1531.0	1502.5		1463.2	+/−	Al_2NO
1495.2	1465.5	−	1431.5	+/−	$Al_x(NO)_y$
1467.1	1442.8		1402.8	+/−	$Al_x(NO)_2$
1421.4	1393.3	−	1364.5	+/−	$Al_x(NO)_y$
1380.6	1353.1	−	1323.7	−/−	$(AlNO)^-$
1364.4	1341.5	−	1305.2	+/−	$(ON)(ON)^-$
1282.1	1263.2	1244.2	1224.5	+/+	AlON
1276.4	1257.8	−	1219.5	−/+	AlON site
1243.7	1218.4	−	1192.0	−/o	NO_2^-
1221.0	1199.9	−	1167.4	−/−	$(NO)_2^-$
1205.3	1181.5	−	1155.5	o/+	NNO_2^-
1176.3	1176.3		1142.1	+/+	Al_2O_2
1129.8	1129.8	−	1100.8	−/+	OAlO
1099.0	1098.8		1063.1	+/	AlOAlN
1079.5	1077.3	1047.5	1044.0	+/−	NAlO
1075.8	1073.3	−	1040.6	+/−	NAlO site
1045.9	1042.9	−	1019.4	−/−	(AlNAlO)
993.0	993.0	−	950.2	−/+	Al_2O
968.4	968.4	−	926.7	+/−	$(Al_2O)(NO)_x$
869.3	852.1		836.6	+/	(AlOAlN)
748.0	741.8	−	−	+/+	aggregates
712.6	704.6	−	699.0	+/+	aggregates
576.4	569.9	−	563.9	−/+	AlON site
566.7	560.9	(560.3)	554.9	+/+	AlON
515.4	511.7	−	503.3	+/−	AlNO site
510.2	506.7	501.4	498.3	+/+	AlNO
496.2	496.2		480.6	+/−	$Al(O_2)$

[a] Annealing/photolysis behavior: + denotes increase, − indicates decrease.

was found for a sharp 1644.3, 1642.6 cm^{-1} doublet. The upper region contained NO and $(NO)_2$ absorptions and new shifted features at 1861.2, 1759.7 cm^{-1} that decreased on annealing and appeared like $(NO)_2$ absorptions in relative intensities. Absorptions for NO_2 and N_2O were also observed because of precursor dissociation and reaction.

Calculations

DFT calculations were performed on potential product molecules using the Gaussian 94 program system.[15] Most calculations employed the hybrid B3LYP functional, but comparisons were done with the BP86 functional as well.[16−18] The 6-311+G* basis set was used for each atom.[19,20] Calculations were done to help identify the molecular species responsible for the 1282.1 and 566.7 cm^{-1} bands, the 1644.3 and 510.2 cm^{-1} absorptions, and the 1079.5 cm^{-1} feature. Because the ^{15}N and ^{18}O shifts for the 1282.1 and 1644.3 cm^{-1} bands suggest the AlON and AlNO arrangements, respectively, both structures must be considered. The small ^{15}N and large ^{18}O shifts for the 1079.5 cm^{-1} absorption indicate an Al−O stretching mode slightly coupled to N so the NAlO insertion product analogous to OAlO must be explored as well.

The energies and structures calculated for the AlNO, AlON, and NAlO isomers in triplet and singlet states are listed in Table 2 for the hybrid B3LYP functional. The Al(NO) cyclic structure was the most stable singlet species; the cyclic triplet had imaginary frequencies. Agreement with the calculations of Ruschel and Ball[3] is reasonable considering the larger basis set employed here. Triplet AlNO is the global minimum at this level of theory, 6.2 kcal/mol below triplet AlON (with ZPE correction this difference is 5.3 kcal/mol). These $^3A''$ states have very little spin contamination. A CCSD(T) calculation was done at the B3LYP minimum structure for triplet AlNO and AlON isomers and the energy difference decreased to 3.8 kcal/mol; it is possible that AlON is in fact the lower energy isomer but a much higher level of theory will be required to answer this question. It is clear that both triplet addition products have nearly the same energy, and that both AlNO and AlON isomers are prepared in the Al + NO matrix reaction reported here.

Frequencies calculated for four isotopic combinations of N and O with ^{27}Al are listed in Table 3. It is immediately seen that the two stretching frequencies calculated for triplet AlNO and for triplet AlON nearly match the positions of two pairs of major product bands, certainly within the range of scaling factors (0.967 for the 1644.3 cm^{-1} band using B3LYP) proposed for DFT calculations.[21] Accordingly, we used the calculated frequencies (unscaled) to compute isotopic ratios for comparison with the observed ratios. The isotopic frequency ratios describe the normal mode and provide a better basis for matching observed and calculated vibrational spectra and thus for identifying new product molecules. Notice in Table 4 that the isotopic ratios for the above five bands are quite different, but that an excellent match is found for triplet AlNO and triplet AlON, and a very good match is found for triplet NAlO.

Similar calculations were done for the doublet anions $AlNO^-$ and $AlON^-$, and the results are given in Tables 2 and 3. Because doublet $AlON^-$ was spin contaminated, quartet $AlON^-$ was also investigated.

Geometries and frequencies calculated with the BP86 functional are listed in Table 5 for the three triplet states. The relative energies and structures are similar to the B3LYP values. The calculated frequencies are slightly different, but in the range expected for DFT. It is perhaps more important to note that isotopic frequency *ratios* (calculated from Table 5) are essentially the same as those found for the B3LYP frequencies for AlNO and NAlO, but the 14/15 ratios (1.01729, 1.00851) and 16/18 ratios (1.02953, 1.01293) calculated from BP86 isotopic frequencies show *less* Al−O−N stretch−stretch interaction than the B3LYP ratios (Table 4) for the AlON isomer.

Calculations were also done for several species containing two NO molecules and a single aluminum atom, and two Al atoms with one NO molecule.[2] The linear doublet Al−Al−NO had a very strong nitrosyl frequency calculated at 1585.9 cm^{-1}. The most stable species with two NO molecules is $^2A_1$ with Al bridging the N−N bond in the *cis*-$(NO)_2$ dimer molecule and strong infrared bands at 1560.4 and 1515.0 cm^{-1}.

Discussion

The new Al, N, O product absorptions will be assigned on the basis of isotopic frequency ratios and agreement with the predictions of DFT calculations.

AlON. The major new product absorption at 1282.1 cm^{-1} dominates the spectrum at higher and lower laser energy/cm^2 so this product most surely contains a single Al atom. It is almost uncanny how close the 1282.1 cm^{-1} band (and 1263.2 and 1224.5 cm^{-1} isotopic counterparts) are to the N_2O fundamental at 1282.7 (and 1263.1 and 1224.0 cm^{-1} isotopic counterparts in solid argon). However, with ±0.1 cm^{-1} accuracy, the 14−16 and 15−18 isotopic product bands are *not* the same as that for N_2O. Furthermore, the stronger 2218.5 cm^{-1} N_2O band was very weak here ($A = 0.004$ AU) and the weaker N_2O band can make less than a 0.001 AU contribution

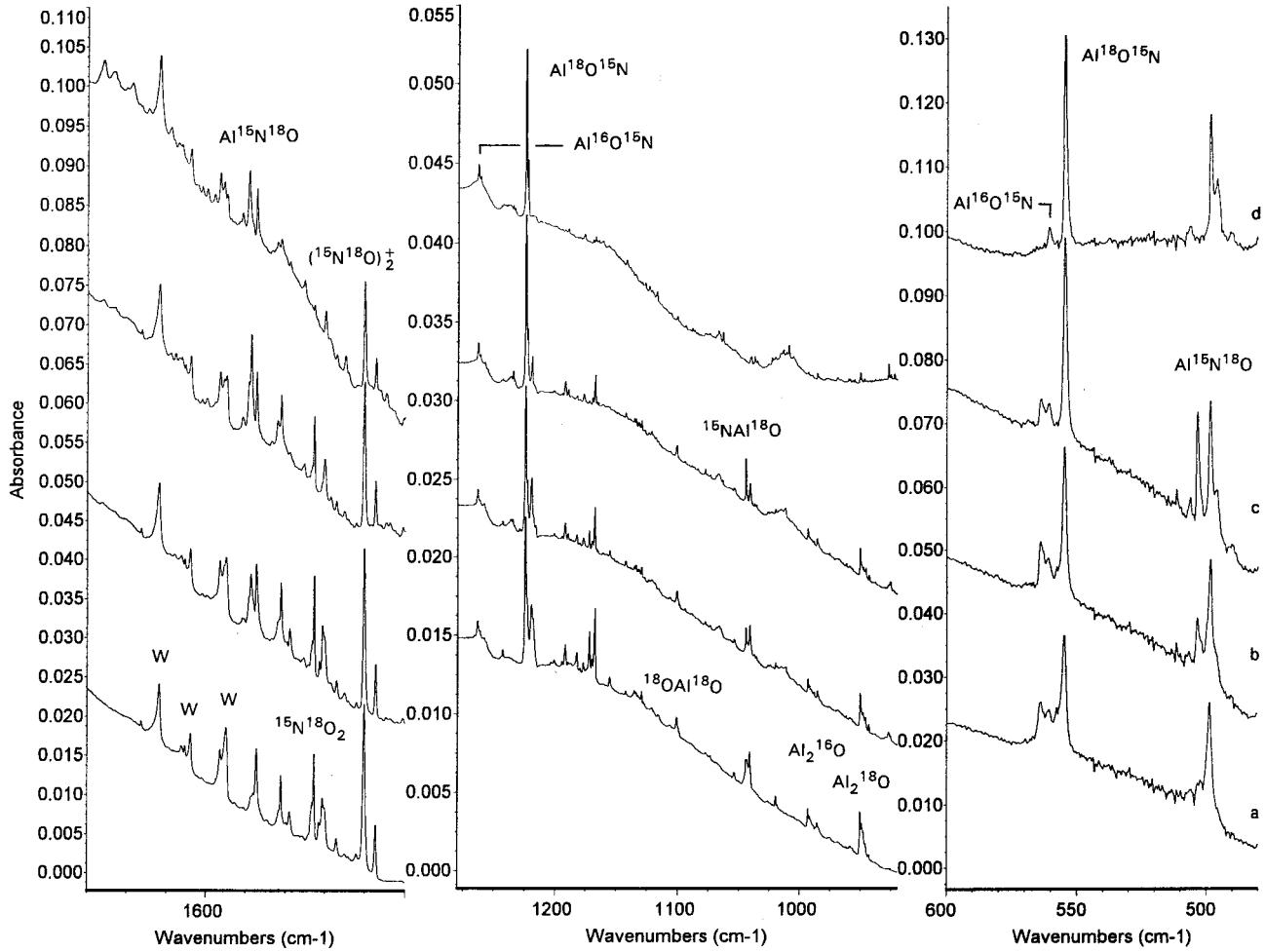

Figure 3. Infrared spectra in selected regions for laser-ablated Al atoms (higher power, 0.2 mm spot) codeposited with 0.4% $^{15}N^{18}O$ in excess argon on a 10 K CsI window; (a) spectrum after 1 h sample codeposition at 10 K, (b) spectrum after annealing to 25 K, (c) spectrum after annealing to 30 K, and (d) spectrum after annealing to 35 K.

at 1283.7 cm^{-1}. Finally, N_2O would give eight isotopic bands with mixed 14, 15, 16, 18 isotopic NO precursors, but only four bands were observed here. Growth on annealing and photolysis (Figure 1) demonstrates that the 566.7 cm^{-1} band and 576.4 cm^{-1} satellite and the 1282.1 cm^{-1} band and 1276.4 cm^{-1} satellite track together and are associated with the same molecular species. Spectra with isotopic mixtures (Figure 4) clearly show that single N and O atom combinations are involved in these molecular vibrations. (The 566.7 cm^{-1} band is *not* due to N_2O.[22]) Thus, the 1282.1 and 566.7 cm^{-1} bands are due to an Al, N, O species.

First, note that the observed 14−16/15−16 and 15−16/15−18 isotopic frequency ratios (Table 4, 1.01496 and 1.03158) show less N and more O participation in this normal mode than the diatomic molecule NO (1.01795 and 1.02772). This suggests a mode where O is moving between two other atoms and the AlON structural arrangement. Further confirmation of this assignment is found in the DFT predicted frequencies at 1277.7 and 545.0 cm^{-1} and the excellent agreement between observed and calculated isotopic frequency ratios for *both* stretching modes of triplet AlON (Table 4), and the lack of agreement for singlet AlON and both AlNO states. In terms of wavenumbers, starting with the $Al^{16}O^{14}N$ band position, DFT predicts the $Al^{16}O^{15}N$ and $Al^{18}O^{15}N$ bands shifted to 1261.9 and 1224.5 cm^{-1} (within 1.3 and 0.0 cm^{-1}) and to 561.1 and 554.8 cm^{-1} (within 0.2 and 0.1 cm^{-1}). Furthermore, two other product bands fit equally well for the AlNO structural isomer.

AlNO. The 1644.3 and 510.2 bands (and 1647.4 and 515.4 cm^{-1} satellites) increase slightly on annealing but decrease on photolysis in concert. Although weaker, these bands are observed in the lowest laser energy investigation, and quartets were observed with the mixed 14, 15, 16, 18 isotopic NO sample, so the AlNO isomer immediately comes to mind. Note for this arrangement that the 14−16/15−16 isotopic frequency ratio is larger and the 15−16/15−18 ratio smaller than diatomic NO values, which requires N to be vibrating between two other atoms. This AlNO assignment is confirmed by the nearby 1699.8 and 496.8 cm^{-1} DFT predicted frequencies *and* the comparison of observed and calculated isotopic ratios for both stretching modes (Table 4), which fit uniquely for triplet AlNO. Again starting with the observed $Al^{14}N^{16}O$ values, DFT predicts $Al^{15}N^{16}O$ and $Al^{15}N^{18}O$ bands shifted to 1612.5 and 1272.8 cm^{-1} (within 0.1 and 1.9 cm^{-1}) and to 507.0 and 498.1 cm^{-1} (within 0.3 and 0.2 cm^{-1}). Furthermore, the calculated relative band intensities (99−133 km/mol) for the two AlNO modes are in reasonable agreement with the observed (0.006−0.012 AU in Figure 1) values. For AlON the calculated relative band intensities (92−123 km/mol) differ more from the observed (0.022−0.012 AU in Figure 1) measurements.

NAlO. The sharp 1079.5, 1075.8 cm^{-1} bands that increase slightly on annealing and decrease slightly on photolysis show small nitrogen (2.2 and 3.5 cm^{-1} for ^{16}O and ^{18}O species) and large oxygen (32.0 and 33.3 cm^{-1} for ^{14}N and ^{15}N species) isotopic shifts. The observed 16/18 ratio 1.03190 is approaching

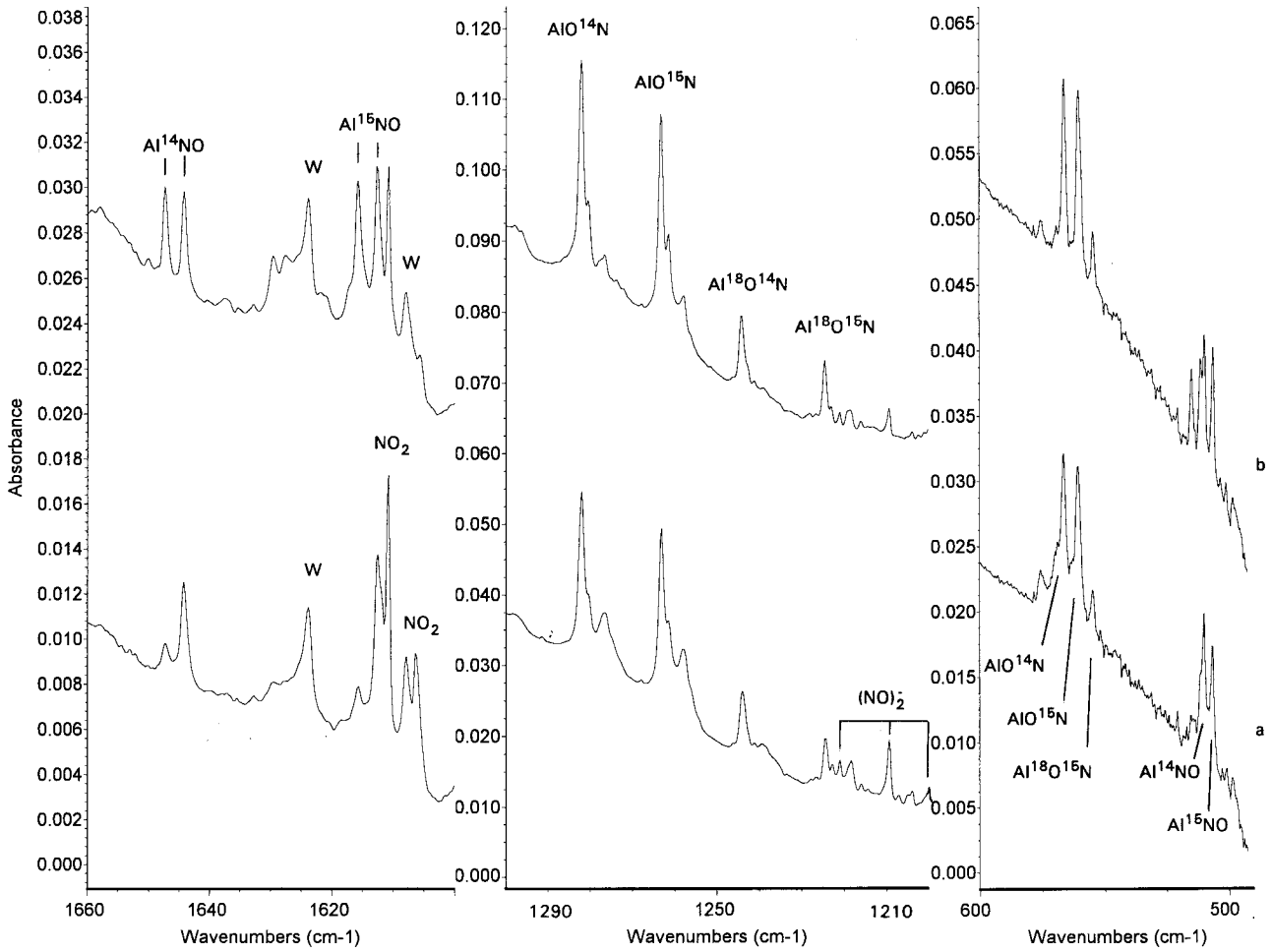

Figure 4. Infrared spectra in selected regions for laser ablated Al atoms (higher power, 0.2 mm spot) codeposited with 0.5% mixed isotopic NO (14:15 = 1:1, 16:18 = 3:1) in excess argon on a 10 K CsI window; (a) spectrum after 1 h sample codeposition at 10 K, and (b) spectrum after annealing to 30 K.

the 1.03689 value calculated for the AlO diatomic molecule, which suggests a mostly terminal Al−O vibration in a molecule with weak coupling to N. The mixed isotopic spectra show resolved pure isotopic bands indicating the involvement of single N and O atoms in this vibration, hence the NAlO insertion product is suggested. The match with B3LYP frequency calculations for triplet NAlO is very good. The Al−N stretching mode calculated to be of comparable intensity near 600 cm^{-1} was not observed. For NFeO, DFT calculations also overestimated the infrared intensity of the M−N stretching vibration.[23]

Other Absorptions. The sharp, weak 1099.0 and 869.3 cm^{-1} bands increase together on annealing in higher laser energy experiments, and the isotopic shifts are appropriate for mixed vibrational modes expected for the secondary reaction product AlOAlN. On the other hand, the weak 1045.9 cm^{-1} band that decreases on annealing is due to a mostly terminal Al−O vibration, and the other isomer AlNAlO is suggested. Frequency calculations at the B3LYP level[2] support these assignments. The 1531.0 cm^{-1} band is relatively weaker in the lower laser power experiments, and the calculated 14/15 (1.01935) and 15/18 (1.02598) isotopic frequency ratios are in good enough agreement with the observed ratios to suggest the AlAlNO assignment. The other bands in Table 1 at 1697.5 cm^{-1} and between 1564.0 and 1421.0 cm^{-1} were produced by annealing and destroyed by photolysis so their identification as $Al_x(NO)_y$ species is clear but specific values of x and y cannot be determined here. Aluminum oxide species and possible NO complexes were detected here. These bands decreased in the series of experiments as the target surface oxide coating was ablated.

Charged Species. Charged species, particularly BO_2^- and O_4^-, have been observed in boron and metal atom laser ablation matrix isolation experiments[6,24,25] so electrons produced by ablation do reach the matrix sample and are captured by molecules during the condensation process. Ionizing radiation is also generated by the focused laser, and this radiation may produce cations in the condensing matrix, as evidenced by the observation of O_4^+ in transition metal experiments.[25]

Nitrogen dioxide is a byproduct in these NO experiments, and NO_2^- is observed at 1243.7 cm^{-1}.[13] Similarly NNO_2^-, a dominant anion in N_2O experiments,[11,13] is detected here at 1205.3 cm^{-1}. A new 1221.0 cm^{-1} band is in fact favored with lower laser energy, a characteristic[25] shared by O_4^-, and this band must be considered for $(NO)_2^-$. The original[11] matrix identification of $(NO)_2^-$ has been revised[12] to $(NO)_2^+$, and an extremely photosensitive species[14] absorbing near 1420 cm^{-1} was not observed here. The 1221.0 cm^{-1} band exhibits diatomic NO isotopic frequency ratios, a triplet with $^{14,15}NO$ and a triplet with $^{15}N^{16,18}O$, and the assignment to $(NO)_2^-$ is proposed. A complete study of this band along with DFT calculations of isotopic frequencies shows that the 1221.0 cm^{-1} band is due to the *trans*-$(NO)_2^-$ isomer.[26]

A weak band at 1364.4 cm^{-1} with low laser energy increases slightly on 25 K annealing, and disappears on photolysis. Based

TABLE 2: Energies and Structures Calculated at the DFT/B3LYP/6-311+G* Level for Low Lying States of Three Al, N, O Isomers and of Two Anion Isomers

state	structure	energy (AU)[a]	bond lengths (Å), angles (deg)
(^{3}A″)[b]	Al−N−O	−372.39493 (E = 0.0)[a]	1.875, 1.201, 175.5
(^{3}A″)[c]	Al−O−N	−372.38508 (E = +6.2)[a]	1.783, 1.279, 179.9
(^{1}A′)[d]	Al(NO)	−372.36480 (E = +18.9)[a]	2.054, 2.042, 1.241
(^{1}A′)[d]	Al−N−O	−372.35551 (E= +24.7)[a]	1.901, 1.191, 165.9
(^{3}A″)[e]	N−Al−O	−372.34000 (E = +34.4)[a]	1.876, 1.616, 180.0
(^{1}A′)[d]	Al−O−N	−372.33107 (E = +40.0)[a]	1.846, 1.236, 179.8
S[f]	N−Al−O	−372.27543 (E = +74.9)[a]	1.820, 1.633, 180.0
D[g]	Al−N−O)$^-$	−372.4316 (E = 23.0)	1.899, 1.207, 174.1
(^{2}A′)[h]	(Al−O−N)$^-$	−372.40011 (E = −3.3)	1.831, 1.278, 179.4
(^{4}A″)[i]	(Al−O−N)$^-$	−372.39609 (E = −0.8)	1.934, 1.281, 135.3

[a] Relative energies (E, kcal/mol). [b] S**2 = 2.0084 before annihilation to 2.0000. [c] S**2 = 2.0078 before annihilation to 2.0000. [d] S**2 = 0.000. [e] S**2 = 2.0149 before annihilation to 2.0001. [f] Unable to determine state, the quintet state is also high energy (E = +73.5)[a] and has 1.963, 1.782 Å bond lengths and 109.2° bond angle. [g] Unable to determine state, S**2 = 0.7849 before annihilation to 0.7503. [h] S**2 = 1.4645 before annihilation to 0.7664. [i] S**2 = 3.7615 before annihilation to 3.7501.

TABLE 3: Isotopic Frequencies and Intensities Calculated (DFT/B3LYP) for the Structures Described in Table 2[a]

	14−16	15−16	14−18	15−18
AlNO	1699.8 (100)	1666.9	1659.6	1625.8
triplet	496.8 (133)	493.7	488.0	485.3
	104.1 (2)	101.6	101.7	100.2
AlON	1277.7 (92)	1257.6	1240.1	1219.1
triplet	545.0 (123)	539.6	538.5	533.7
	116.0 (2)	115.1	111.5	110.6
AlNO	1706.0 (266)	1674.0	1663.8	1630.9
singlet	473.8 (86)	469.8	466.8	463.0
	107.3 (10)	104.9	105.8	103.4
Al(NO)	1468.6 (54)	1442.7	1429.6	1402.9
singlet	485.8 (58)	475.4	485.1	474.7
	374.1 (41)	373.1	360.3	359.4
NAlO	1079.8 (3)	1079.2	1047.1	1046.3
triplet	605.9 (6)	590.9	599.3	584.4
	176.2 (93)	174.9	173.7	172.4
AlON	1356.5 (81)	1332.3	1321.1	1296.0
singlet	454.4 (55)	450.9	447.5	444.5
	146.2 (1)	145.0	140.6	139.3
NAlO	1031.3 (19)	1030.0	1003.2	1001.5
singlet	681.6 (17)	665.2	672.0	655.9
	177.3 (199)	176.0	174.9	173.5
(AlNO)$^-$	1430.7 (697)	1401.9	1399.3	1369.6
doublet	586.5 (40)	583.3	575.1	572.5
	273.3 (57)	266.7	270.0	263.3
(AlON)$^-$	1237.2 (125)	1215.4	1204.4	1181.8
doublet	434.5 (4)	431.1	428.1	425.1
	122.5 (1)	121.5	117.1	116.7
(AlON)$^-$	1302.7 (100)	1279.4	1268.5	1244.5
quartet	425.5 (118)	424.0	414.2	412.9
	214.3 (4)	211.3	209.0	206.1

[a] Frequencies, cm^{-1} (intensities, km/mol).

on isotopic ratios (1.01707, 1.02781), the 1364.4 cm^{-1} band is appropriate for NO$^-$, which has been observed at 1353−1374 cm^{-1} in the matrix isolated (M^+)(NO^-) species.[11,13,14,27] However, the annealing behavior suggests a cluster ion (ON)(ON)$^-$ as is discussed in detail.[26]

TABLE 4: Comparison of Observed and Calculated (DFT/B3LYP) Isotopic Frequency Ratios for Stretching Fundamentals of AlNO, AlON, and NAlO in Triplet and Singlet States

	14−16/15−16			15−16/15−18		
	obs	calc T	calc S	obs	calc T	calc S
AlNO	1.01966	1.01974	1.01912	1.02407	1.02530	1.02643
	1.00691	1.00628	1.00851	1.01686	1.01731	1.01469
AlON	1.01496	1.01598	1.01816	1.03160	1.03158	1.02801
	1.01034	1.01000	1.00776	1.01081	1.01105	1.01440
NAlO	1.00204	1.00056	1.00126	1.03190	1.03144	1.02845

TABLE 5: Structures, Frequencies, and Intensities Calculated at the DFT/BP86/6-311+G* Level for Triplet States of Three Al, N, O Isomers

	14−16	15−16	14−18	15−18
AlNO[a]	1629.1 (171)	1598.0	1589.9	1557.9
1.899, 1.207 Å	470.1 (93)	467.0	462.0	459.4
174.1°	101.7 (2)	101.2	102.2	99.7
AlON[a]	1223.6 (0.4)	1202.8	1189.9	1168.3
1.818, 1.273 Å	497.6 (80)	493.4	490.8	487.1
180.0°	143.6 (2)	142.4	138.1	136.9
NAlO[a]	985.4 (18)	948.9	955.7	954.9
1.870, 1.644 Å	600.8 (21)	585.9	594.2	579.4
179.7°	158.1 (78)	156.9	155.9	154.7

[a] Relative energies (kcal/mol): AlNO (E = 0.0), AlON (E = +10.0), NAlO (E = +36.5).

The weak band at 1380.6 cm^{-1} in the higher laser energy experiment with half the absorbance of the 1644.3 cm^{-1} band decreased on annealing and photolysis but was favored relative to the 1644.3 cm^{-1} band with lower laser energy *while the yield of charged species increased*. DFT calculations predict the strongest (×17) band of doublet AlNO$^-$ at 1430.7 cm^{-1} with 14−16/15−16 isotopic frequency ratio 1.02054 and 15−16/15−18 ratio 1.02358, which are in excellent agreement with the observed 1.02032 and 1.02221 ratios. Accordingly, the 1380.6 cm^{-1} band is assigned to AlNO$^-$. Although the total yield of AlON in these experiments appeared to exceed the yield of AlNO (estimated ×5 based on integrated band intensities and comparable calculated infrared intensities), no evidence was found for the AlON$^-$ anion species based on calculated frequencies and isotopic shifts. The total electronic energy of doublet AlNO$^-$ is 23.0 kcal/mol below that for triplet AlNO, which is appropriate for the electron affinity of AlNO$^-$. Note that the electron affinity of NO is lower (0.4 kcal/mol)[28] but the electron affinity of AlO is higher (60.0 kcal/mol).[29]

Reaction Mechanisms. The reaction mechanism is of interest particularly in view of formation of the NAlO insertion product only in laser ablation experiments and of both AlNO and AlON addition products in thermal and laser-ablated Al atom experiments. Because AlNO and AlON absorptions both increase (30−40%) on annealing from 10 to 25 K (see Figure 2), the addition reaction 1 must proceed with little or no activation energy.

$$\mathrm{Al} + \mathrm{NO} \rightarrow \mathrm{AlNO\ and\ AlON} \qquad (1)$$

Although broadband photolysis appears to affect the satellite bands (Figure 1), the major absorptions for AlNO and AlON are only slightly increased by photolysis (10 and 3%, respectively). The higher energy singlet cyclic Al(NO) species is not observed here.

The NAlO insertion product is observed only in laser ablation experiments with higher laser power so activation energy must be required. Considerable excess energy (>5 eV)[30,31] is present in the Al atoms ablated here with higher laser power.

$$Al + NO \xrightarrow{E_a} NAlO \quad (2)$$

The slight growth of NAlO on annealing must then be due to diffusion and reaction of N and O atoms; the N_2O and NO_2 absorptions increased on the first annealing cycle presumably because of atom reactions with NO. Note that the experiment with a 2 mm diameter laser focal point failed to produce the insertion product, but both addition products were observed.

Anions are formed in these experiments by capture of electrons from the laser ablation process. The observation of NO_2^-, NNO_2^-, and a new $(NO)_2^-$ isomer attest to this fact. Calculations suggest that the most stable aluminum-containing anion in these experiments is $AlNO^-$, and this anion is also formed by electron capture. The $AlNO^-$ species is destroyed by broadband photolysis, consistent with the 23.0 kcal/mol electron affinity suggested by DFT calculations.

$$Al + NO + e \rightarrow AlNO^- \quad (3)$$

Conclusions

Laser-ablated aluminum atoms react with NO, ^{15}NO, and $^{15}N^{18}O$ during condensation in excess argon using different concentrations and laser energies/cm^2. The isotopic frequency ratios characterize different normal modes, and these are uniquely matched to the stretching modes of triplet AlON (1282.1, 566.7 cm^{-1}) and triplet AlNO (1644.3, 510.2 cm^{-1}) by DFT isotopic frequency calculations. The fifth band (1079.5 cm^{-1}) is due to a terminal Al−O stretching mode that is consistent with triplet NAlO based on DFT isotopic frequency calculations. The total product yield depended on laser energy; both AlON and AlNO addition products were produced with lower energy, but the insertion product NAlO required higher energy. Anions were favored with lower laser energy, and a weak 1380.6 cm^{-1} band is assigned to $AlNO^-$ in accord with DFT isotopic frequency calculations.

Acknowledgment. We are grateful for N.S.F. support under grant CHE 97-00116 for this research and for helpful correspondence with D. W. Ball.

References and Notes

(1) Mroz, T. J., Jr. *Ceram. Bull.* **1991**, *70*, 849.
(2) Andrews, L.; Bare, W. D.; Chertihin, G. V.; Hannachi, Y., submitted for publication.
(3) Ruschel, G. K.; Ball, D. W. *High Temp. Mater. Sci.* **1997**, *37*, 63. At our request, D. W. Ball remeasured the strongest product band reported at 1285 cm^{-1} and refined the measurement to 1282 cm^{-1}.
(4) At our request, D. W. Ball checked his original spectra from thermal Al + NO experiments and found a weak band at 1644 cm^{-1} in the water region and weak bands at 566 and 510 cm^{-1} in the region made very noisy by the ZnSe optical cutoff. Although it is difficult to compare band absorbances recorded under different experimental conditions, the relative intensities of the 1644, 1282, 566, and 510 cm^{-1} bands in the thermal and laser-ablated Al + NO experiments appear to be approximately the same. No absorption was observed at 1079, 1075 cm^{-1} in the thermal study.
(5) Andrews, W. L. S.; Pimentel, G. C. *J. Chem. Phys.* **1965**, *44*, 2361.
(6) Andrews, L.; Burkholder, T. R.; Yustein, J. T. *J. Phys. Chem.* **1992**, *96*, 10182.
(7) Chertihin, G. V.; Andrews, L. *J. Phys. Chem.* **1993**, *97*, 10295.
(8) Chertihin, G. V.; Andrews, L.; Taylor, P. R. *J. Am. Chem. Soc.* **1994**, *116*, 3513.
(9) Lanzisera, D. V.; Andrews, L. *J. Phys. Chem. A* **1997**, *101*, 5082.
(10) Lanzisera, D. V.; Andrews, L. *J. Phys. Chem. A* **1997**, *101*, 9660.
(11) Hacaloglu, J.; Suzer, S.; Andrews, L. *J. Phys. Chem.* **1990**, *94*, 1759.
(12) Strobel, A.; Knoblauch, N.; Agreiter, J.; Smith, A. M.; Neider-Schatteburg, G.; Bondybey, V. E. *J. Phys. Chem.* **1995**, *99*, 872.
(13) Milligan, D. E.; Jacox, M. E. *J. Chem. Phys.* **1971**, *55*, 3404.
(14) Jacox, M. E.; Thompson, W. E. *J. Chem. Phys.* **1990**, *93*, 7609.
(15) Frisch, M. J.; Trucks, G. W.; Schlegel, H. B.; Gill, P. M. W.; Johnson, B. G.; Robb, M. A.; Cheeseman, J. R.; Keith, T.; Petersson, G. A.; Montgomery, J. A.; Raghavachari, K.; Al-Laham, M. A.; Zakrzewski, V. G.; Ortiz, J. V.; Foresman, J. B.; Cioslowski, J.; Stefanov, B. B.; Nanayakkara, A.; Challacombe, M.; Peng, C. Y.; Ayala, P. Y.; Chen, W.; Wong, M. W.; Andres, J. L.; Replogle, E. S.; Gomperts, R.; Martin, R. L.; Fox, D. J.; Binkley, J. S.; Defrees, D. J.; Baker, J.; Stewart, J. P.; Head-Gordon, M.; Gonzalez, C.; Pople J. A. *Gaussian 94, Revision B.1*; Gaussian, Inc.: Pittsburgh, PA, 1995.
(16) Lee, C.; Yang, E.; Parr, R. G. *Phys. Rev. B* **1988**, *37*, 785.
(17) Perdew, J. P. *Phys. Rev. B* **1986**, *33*, 8822.
(18) Becke, A. D. *J. Chem. Phys.* **1993**, *98*, 5648.
(19) McLean, A. D.; Chandler, G. S. *J. Chem. Phys.* **1980**, *72*, 5639.
(20) Krishnan, R.; Binkley, J. S.; Seeger, R.; Pople, J. A. *J. Chem. Phys.* **1980**, *72*, 650.
(21) Scott, A. P.; Random, L. *J. Phys. Chem.* **1996**, *100*, 16502.
(22) Smith, D. Foss, Jr.; Overend, J.; Spiker, R. C.; Andrews, L. *Spectrochim. Acta* **1972**, *28A*, 87.
(23) Chertihin, G. V.; Andrews, L.; Neurock, M. *J. Phys. Chem.* **1996**, *100*, 14609.
(24) Burkholder, T. R.; Andrews, L. *J. Chem. Phys.* **1991**, *95*, 8697.
(25) Chertihin, G. V.; Saffell, W.; Yustein, J. T.; Andrews, L.; Neurock, M.; Ricca, A.; Bauschlicher, C. W., Jr. *J. Phys. Chem.* **1996**, *100*, 5261.
(26) Andrews, L.; Zhou, M. F.; Willson, S. P.; Kushto, G. P.; Snis, A.; Panas, I. *J. Chem. Phys.* **1998**, *109*.
(27) Tevault, D. E.; Andrews, L. *J. Phys. Chem.* **1973**, *77*, 1646.
(28) Spence, D.; Schulz, G. *J. Phys. Rev. A* **1971**, *3*, 1968.
(29) Desai, S. R.; Wu, H.; Rohfling, C.; Wang, L. S. *J. Chem. Phys.* **1997**, *106*, 1309.
(30) Kang, H.; Beauchamp, J. L. *J. Phys. Chem.* **1985**, *89*, 3364.
(31) Salzberg, A. P.; Santiago, D. I.; Asmar, F.; Sandoval, D. N.; Weiner, B. R. *Chem. Phys. Lett.* **1991**, *180*, 161. Wang, H.; Salzberg, A. P.; Weiner, B. R. *Appl. Phys. Lett.* **1991**, *59*, 935.